From proteins to polysaccharides: lifestyle and genetic evolution of *Coprothermobacter proteolyticus*.

B.J. Kunath[1#], F. Delogu[1#], M.Ø. Arntzen[1], V.G.H. Eijsink[1], T.R. Hvidsten[1], P.B. Pope[1*]

1. Faculty of Chemistry, Biotechnology and Food Science, Norwegian University of Life Sciences, 1432 Ås, NORWAY.

[#] **Equal contributors**

***Corresponding Author:** Phillip B. Pope
Faculty of Chemistry, Biotechnology and Food Science
Norwegian University of Life Sciences
Post Office Box 5003
1432, Ås, Norway
Phone: +47 6496 6232
Email: phil.pope@nmbu.no

RUNNING TITLE:

The genetic plasticity of *Coprothermobacter*

COMPETING INTERESTS

The authors declare there are no competing financial interests in relation to the work described.

KEYWORDS

CAZymes; Horizontal gene transfer; strain heterogeneity; Metatranscriptomics

ABSTRACT

Microbial communities that degrade lignocellulosic biomass are typified by high levels of species- and strain-level complexity as well as synergistic interactions between both cellulolytic and non-cellulolytic microorganisms. *Coprothermobacter proteolyticus* frequently dominates thermophilic, lignocellulose-degrading communities with wide geographical distribution, which is in contrast to reports that it ferments proteinaceous substrates and is incapable of polysaccharide hydrolysis. Here we deconvolute a highly efficient cellulose-degrading consortium (SEM1b) that is co-dominated by *Clostridium (Ruminiclostridium) thermocellum*- and multiple heterogenic strains affiliated to *C. proteolyticus.* Metagenomic analysis of SEM1b recovered metagenome-assembled genomes (MAGs) for each constituent population, whilst in parallel two novel strains of *C. proteolyticus* were successfully isolated and sequenced. Annotation of all *C. proteolyticus* genotypes (two strains and one MAG) revealed their genetic acquisition of various carbohydrate-active enzymes (CAZymes), presumably derived from horizontal gene transfer (HGT) events involving *C. thermocellum*- or Thermotogae-affiliated populations that are historically co-located. HGT material included whole saccharolytic operons and dockerin-encoding enzymatic subunits that are synonymous with cellulosomes. Finally, temporal genome-resolved metatranscriptomic analysis of SEM1b revealed expression of *C. proteolyticus* CAZymes at different SEM1b life-stages as well as co-expression of CAZymes from multiple SEM1b populations, inferring deeper microbial interactions that are dedicated towards co-degradation of cellulose and hemicellulose. We show that *C. proteolyticus*, a ubiquitous keystone population, consists of closely related strains that have adapted via HGT to degrade both oligo- and longer polysaccharides present in decaying plants and microbial cell walls, thus explaining its dominance in thermophilic anaerobic digesters on a global scale.

63 **INTRODUCTION**

64 The anaerobic digestion of plant biomass profoundly shapes innumerable ecosystems,
65 ranging from the gastrointestinal tracts of humans and other mammals to those that drive
66 industrial applications such as biofuel generation. Biogas reactors are one of the most
67 commonly studied anaerobic systems, yet many keystone microbial populations and their
68 metabolic processes are poorly understood due to a lack of cultured or genome sampled
69 representatives. *Coprothermobacter* spp. are frequently observed in high abundance in
70 thermophilic anaerobic systems, where they are believed to exert strong protease activity
71 whilst generating hydrogen and acetate, key intermediate metabolites for biogas production
72 (Tandishabo *et al.,* 2012). Molecular techniques have shown that their levels range from 10
73 to 90% of the total microbial community, irrespective of bioreactors being operated on
74 lignocellulose- or protein-rich substrates (**Figure 1**). Despite their promiscuous distribution,
75 global abundance and key role in biogas production, only two species have been described:
76 *Coprothermobacter platensis* (Etchebehere *et al.,* 1998) and *Coprothermobacter proteolyticus*
77 (Ollivier *et al.,* 1985). These two species and their inherent phenotypes have formed the
78 predictive basis for the majority of *Coprothermobacter*-dominated systems described to
79 date. Recent studies have illustrated that *C. proteolyticus* populations in anaerobic biogas
80 reactors form cosmopolitan assemblages of closely related strains that are hitherto
81 unresolved (Hagen *et al.,* 2017).

82

83 Frequently in nature, microbial populations are composed of multiple strains with genetic
84 heterogeneity (Kashtan *et al.,* 2014, Schloissnig *et al.,* 2013). Studies of strain-level
85 populations have been predominately performed with the human microbiome and
86 especially the gut microbiota (Bron *et al.,* 2012, Spanogiannopoulos *et al.,* 2016). The reasons
87 for strain diversification and their coexistence remain largely unknown (Ellegaard and Engel
88 2016), however several mechanisms have been hypothesized, such as: micro-niche selection
89 (Hunt *et al.,* 2008, Kashtan *et al.,* 2014), host selection (McLoughlin *et al.,* 2016), cross-feed
90 interactions (Rosenzweig *et al.,* 1994, Zelezniak *et al.,* 2015) and phage selection (Rodriguez-
91 Valera *et al.,* 2009). Studies of isolated strains have shown that isolates can differ in a
92 multitude of ways, including virulence and drug resistance (Gill *et al.,* 2005, Sharon *et al.,*
93 2013, Solheim *et al.,* 2009), motility (Zunino *et al.,* 1994) and nutrient utilization (Siezen *et*

94 *al.,* 2010). Strain-level genomic variations typically consist of single-nucleotide variants
95 (SNVs) as well as acquisition/loss of genomic elements such as genes, operons or plasmids
96 via horizontal gene transfer (HGT) (Koskella and Vos 2015, Tettelin *et al.,* 2005, Treangen
97 and Rocha 2011). Variability in gene content caused by HGT is typically attributed to phage-
98 related genes and other genes of unknown function (Ochman *et al.,* 2000), and can give rise
99 to ecological adaptation, niche differentiation and eventually speciation (Bendall *et al.,* 2016,
100 Biller *et al.,* 2015, Shapiro *et al.,* 2012). Although differences in genomic features can be
101 accurately characterized in isolated strains, it has been difficult to capture such information
102 using culture-independent approaches such as metagenomics. Advances in bioinformatics
103 have improved taxonomic profiling of microbial communities from phylum to species level
104 but it remains difficult to profile similar strains from metagenomes and compare them with
105 the same level of resolution obtained by comparison of isolate genomes (Truong *et al.,* 2017).
106 Since closely-related strains can also differ in gene expression (González-Torres *et al.,* 2015),
107 being able to distinguish the expression profiles of individual strains in a broader ecological
108 context is elemental to understanding the influence they exert towards the overall
109 community function.
110
111 In this study, a novel population of *C. proteolyticus* that included multiple closely related
112 strains, was observed within a simplistic biogas-producing consortium enriched on cellulose
113 (hereafter referred to as SEM1b). Using a combined metagenomic and culture-dependent
114 approach, two strains and a metagenome-assembled genome (MAG) affiliated to *C.*
115 *proteolyticus* were recovered and genetically compared to the only available type strain, *C.*
116 *proteolyticus* DSM 5265 (Alexiev *et al.,* 2014). Notable genomic differences included the
117 acquisition of carbohydrate-active enzymes (CAZymes), which inferred that *C. proteolyticus*
118 has adapted to take advantage of lignocellulosic polysaccharides. We further examined the
119 saccharolytic potential of our recovered *C. proteolyticus* population in a broader community
120 context, by examining genome-resolved temporal metatranscriptomic data generated from
121 the SEM1b consortium. Collective analysis highlighted the time-specific polysaccharide-
122 degrading activity that *C. proteolyticus* exerts in a cellulolytic microbial community.
123

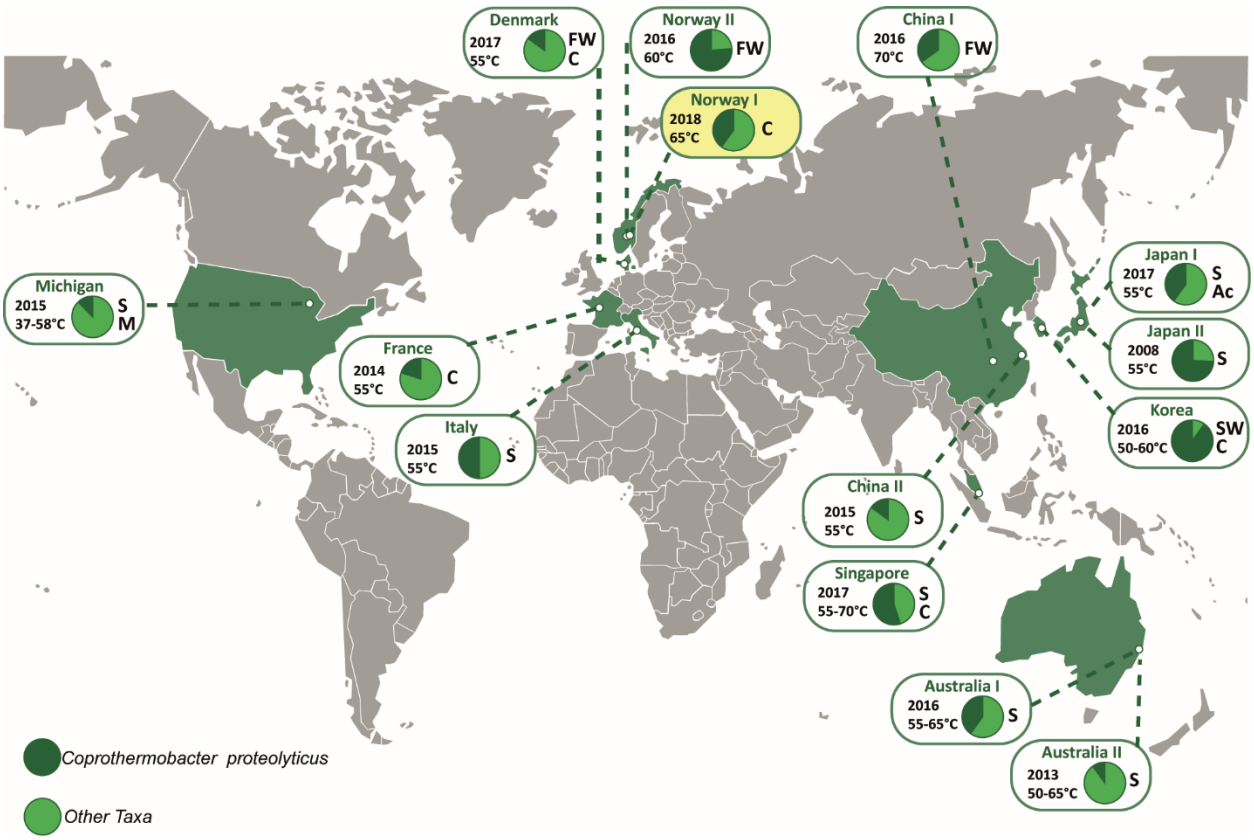

Figure 1. Global distribution of *Coprothermobacter proteolyticus*-affiliated populations in anaerobic biogas reactors. Charts indicate relative 16S rRNA gene abundance of OTUs affiliated to *C. proteolyticus* (dark green), in comparison to the total community (light green). The year of publication, reactor temperature and substrate (C: cellulose, FW: food waste, S: sludge, SW: Seaweed, Ac: acetate) is indicated (details in **Table S1**). The SEM1b consortium analyzed in this study is highlighted in yellow.

MATERIALS AND METHODS

Origin of samples and generation of the SEM1b consortium

An inoculum (100µl) was collected from a lab-scale biogas reactor (Reactor TD) fed with manure and food waste and run at 55°C. The TD reactor originated itself from a thermophilic biogas plant (Frevar) fed with food waste and manure in Fredrikstad, Norway. Our research groups have previously studied the microbial communities in both the Frevar plant (Hagen *et al.,* 2017) and the TD bioreactor (Zamanzadeh *et al.,* 2016), which provided a detailed understanding of the original microbial community. The inoculum was transferred for serial dilution and enrichment to an anaerobic serum bottle incubated at 65°C and containing the rich ATCC medium 1943, with cellobiose substituted for 10g/L of cellulose in the form of

141 BALI treated Norway spruce (Rødsrud *et al.,* 2012). After an initial growth cycle, an aliquot
142 was removed and serially diluted to extinction. Briefly, a 100µl sample was transferred to a
143 new bottle of anaerobic medium, mixed and 100µl was directly transferred again to a new
144 one (six serial transfers in total). The consortium at maximum dilution that retained the
145 cellulose-degrading capability (SEM1b) was retained for the present work, and aliquots
146 were stored at – 80°C with glycerol (15% v/v). In parallel, continuous SEM1b cultures were
147 maintained via regular transfers into fresh media (each generation incubated for ~2-3 days).
148

149 **Metagenomic analysis**

150 Two different samples (D1B and D2B) were taken from a continuous SEM1b culture and
151 were used for shotgun metagenomic analysis. D2B was 15 generations older than D1B and
152 was used to leverage improvements in metagenome assembly and binning. From 6ml of
153 culture, cells were pelleted by centrifugation at 14000 x *g* for 5 minutes and were kept frozen
154 at -20°C until processing. Non-invasive DNA extraction methods were used to extract high
155 molecular weight DNA as previously described (Kunath *et al.,* 2017). The DNA was quantified
156 using a Qubit™ fluorimeter and the Quant-iT™ dsDNA BR Assay Kit (Invitrogen, USA) and the
157 quality was assessed with a NanoDrop 2000 (Thermo Fisher Scientific, USA).
158

159 16S rRNA gene analysis was performed on both D1B and D2B samples. The V3-V4 hyper-
160 variable regions of bacterial and archaeal 16S rRNA genes were amplified using the
161 341F/805R primer set: 5'-CCTACGGGNBGCASCAG-3' / 5'-GACTACNVGGGTATCTAATCC-3'
162 (Takahashi *et al.,* 2014). The PCR was performed as previously described (Zamanzadeh *et*
163 *al.,* 2016) and the sequencing library was prepared using Nextera XT Index kit according to
164 Illumina's instructions for the MiSeq system (Illumina Inc.). MiSeq sequencing (2x300bp
165 with paired-ends) was conducted using the MiSeq Reagent Kit v3. The reads were quality
166 filtered (Phred ≥ Q20) and USEARCH61 (Edgar 2010) was used for detection and removal of
167 chimeric sequences. Resulting sequences were clustered at 97% similarity into operational
168 taxonomic units (OTUs) and taxonomically annotated with the
169 pick_closed_reference_otus.py script from the QIIME v1.8.0 toolkit (Caporaso *et al.,* 2010)
170 using the Greengenes database (gg_13_8). The resulting OTU table was corrected based on
171 the predicted number of *rrs* operons for each taxon (Stoddard *et al.,* 2015).

172

173 D1B and D2B were also subjected to metagenomic shotgun sequencing using the Illumina
174 HiSeq3000 platform (Illumina Inc) at the Norwegian Sequencing Center (NSC, Oslo, Norway).
175 Samples were prepared with the TrueSeq DNA PCR-free preparation, and sequenced with
176 paired-ends (2x125bp) on four lanes (two lanes per sample). Quality trimming of the raw
177 reads was performed using cutadapt (Martin 2011), removing all bases on the 3' end with a
178 Phred score lower than 20 (if any present) and excluding all reads shorter than 100nt,
179 followed by a quality filtering using the FASTX-Toolkit (http://hannonlab.cshl.edu/fastx_toolkit/).
180
181 Reads with a minimum Phred score of 30 over 90% of the read length were retained.
182 In addition, genomes from two isolated *C. proteolyticus* strains (see below) were used to
183 decrease the data complexity and to improve the metagenomic assembly and binning. The
184 quality-filtered metagenomic reads were mapped against the assembled strains using the
185 BWA-MEM algorithm requiring 100% identity (Li 2013). Reads that mapped the strains
186 were removed from the metagenomic data and the remaining reads were co-assembled
187 using MetaSpades v3.10.0 (Nurk *et al.,* 2017) with default parameters and k-mer sizes of 21,
188 33, 55 and 77. The subsequent contigs were binned with Metabat v0.26.3 (Kang *et al.,* 2015)
189 in "very sensitive mode", using the coverage information from D1B and D2B. The quality
190 (completeness, contamination and strain heterogeneity) of the bins (hereafter referred to as
MAGs) was assessed by CheckM v1.0.7 (Parks *et al.,* 2015) with default parameters.
191

192 **Isolation of *C. proteolyticus* strains**

193 Strains were isolated using the Hungate method (Hungate 1969). In brief: Hungate tubes
194 were anaerobically prepared with the DSMZ medium 481 with and without agar (15g/L).
195 Directly after being autoclaved, Hungate tubes containing agar were cooled down to 65°C
196 and sodium sulfide nonahydrate was added. From the SEM1b culture used for D1B, 100µl
197 were transferred to a new tube and mixed. From this new tube, 100µl was directly
198 transferred to fresh medium, mixed and transferred again (six transfers in total). Tubes were
199 then cooled to 60°C for the agar to solidify, and then kept at the same temperature. After
200 growth, single colonies were picked and transferred to liquid medium.
201

202 DNA was extracted using the aforementioned method for metagenomic DNA, with one
203 amendment: extracted DNA was subsequently purified with DNeasy PowerClean Pro
204 Cleanup Kit (Qiagen, USA) following manufacturer's instructions. To insure the purity of the
205 *C. proteolyticus* colonies, visual confirmation was performed using light microscopy and long
206 16S rRNA genes were amplified using the primers pair 27F/1492R (Schumann 1991): 5'-
207 AGAGTTTGATCMTGGCTCAG-3' / 5'-TACGGYTACCTTGTTACGACTT-3' and sequenced using
208 Sanger technology. The PCR consisted of an initial denaturation step at 94°C for 5 min and
209 30 cycles of denaturation at 94°C for 1 min, annealing at 55°C for 1 min, and extension at
210 72°C for 1 min, and a final elongation at 72°C for 10 min. PCR products were purified using
211 the NucleoSpin Gel and PCR Clean-up kit (Macherey-Nagel, Germany) and sent to GATC
212 Biotech for Sanger sequencing.
213
214 The genomes of two isolated *C. proteolyticus* strains (hereafter referred to as *BWF2A* and
215 *SW3C*) were sequenced at the Norwegian Sequencing Center (NSC, Oslo, Norway). Samples
216 were prepared with the TrueSeq DNA PCR-free preparation and sequenced using paired-
217 ends (2x300bp) on a MiSeq system (Illumina Inc). Quality trimming, filtering and assembly
218 were performed as described in the aforementioned metagenomic assembly section. All
219 contigs from the strains and the Metagenome Assembled Genomes (MAGs) were submitted
220 to the Integrated Microbial Genomes and Microbiomes (IMG/M) system (Chen *et al.,* 2017)
221 for genomic feature prediction and annotation (pipeline version 4.15.1). Resulting annotated
222 open reading frames (ORFs) were retrieved, further annotated for carbohydrate-active
223 enzymes (CAZymes) using dbCAN HMMs v5.0 (Yin *et al.,* 2012), and subsequently used as a
224 reference database for the metatranscriptomics. The genomes for both Strains and MAGs
225 corresponding to *C. proteolyticus* were compared to the reference genome from *C.*
226 *proteolyticus* DSM 5265 (Accession number: CP001145, Alexiev *et al.,* 2014). Using the BRIG
227 tool (Alikhan *et al.,* 2011) for mapping and visualization, the different genomes were mapped
228 against their pan genome generated using Roary (Page *et al.,* 2015).
229
230 **Phylogenetic analysis**
231 A concatenated ribosomal protein phylogeny was performed on the MAGs and the isolated
232 strains using 16 ribosomal proteins chosen as single-copy phylogenetic marker genes (RpL2,

233 3, 4, 5, 6, 14, 15, 16, 18, 22 and 24, and RpS3, 8, 10, 17 and 19) (Hug *et al.,* 2016). The dataset
234 was augmented with metagenomic sequences retrieved from our previous research on the
235 original FREVAR reactor (Hagen *et al.,* 2017) and with sequences from reference genomes
236 identified during the 16S rRNA analysis. Each gene set was individually aligned using
237 MUSCLE v3.8.31 (Edgar 2004) and then manually curated to remove end gaps and
238 ambiguously aligned terminal regions. The curated alignments were concatenated and a
239 maximum likelihood phylogeny was obtained using MEGA7 (Kumar *et al.,* 2016) with 1000
240 bootstrap replicates. The radial tree was visualized using iTOL (Letunic and Bork 2016).
241 Additionally, an average nucleotide identity (ANI) comparison was performed between each
242 MAG and their closest relative using the ANI calculator (Rodriguez-R and Konstantinidis
243 2016).
244
245 **Temporal meta-omic analyses of SEM1b**
246 A "meta-omic" time series analysis was conducted over the lifetime span of the SEM1b
247 consortium (≈45hours). A collection of 27 replicate bottles containing ATCC medium 1943
248 with 10g/L of cellulose, were inoculated from the same SEM1b culture, and incubated at 65°C
249 in parallel. For each sample time point, three culture-containing bottles were removed from
250 the collection and processed in triplicate. Sampling occurred over nine time-points (at 0, 8,
251 13, 18, 23, 28, 33, 38 and 43 hours) during the SEM1b life-cycle, and are hereafter referred
252 as T0, T1, T2, T3, T4, T5, T6, T7 and T8, respectively. DNA for 16S rRNA gene analysis was
253 extracted (as above) from T1 to T8 and kept at -20°C until amplification and sequencing, and
254 the analysis was performed using the protocol described above. Due to low cell biomass at
255 the initial growth stages, sampling for metatranscriptomics was performed from T2 to T8.
256 Sample aliquots (6 ml) were treated with RNAprotect Bacteria Reagent (Qiagen, USA)
257 following the manufacturer's instructions and the treated cell pellets were kept at -80°C until
258 RNA extraction.
259
260 In parallel, metadata measurements including cellulose degradation rate, monosaccharide
261 production and protein concentration were performed over all the nine time points (T0-T8).
262 For monosaccharide detection, 2 ml samples were taken in triplicates, centrifuged at 16000
263 x *g* for 5 minutes and the supernatants were filtered with 0.2µm sterile filters and boiled for

264 15 minutes before being stored at -20°C until processing. Solubilized sugars released during
265 microbial hydrolysis were identified and quantified by high-performance anion exchange
266 chromatography (HPAEC) with pulsed amperiometric detection (PAD). A Dionex ICS3000
267 system (Dionex, Sunnyvale, CA, USA) equipped with a CarboPac PA1 column (2 × 250 mm;
268 Dionex, Sunnyvale, CA, USA), and connected to a guard of the same type (2 × 50 mm), was
269 used. Separation of products was achieved using a flow rate of 0.25 mL/min in a 30-minute
270 isocratic run at 1 mM KOH at 30°C. For quantification, peaks were compared to linear
271 standard curves generated with known concentrations of selected monosaccharides
272 (glucose, xylose, mannose, arabinose and galactose) in the range of 0.001-0.1 g/L.
273
274 Total proteins measurements were taken to estimate SEM1b growth rate. Proteins were
275 extracted following a previously described method (Hagen *et al.,* 2017) with a few
276 modifications. Briefly, 30ml culture aliquots were centrifuged at 500 x *g* for 5 minutes to
277 remove the substrate and the supernatant was centrifuged at 9000 x *g* for 15 minutes to
278 pellet the cells. Cell lysis was performed by resuspending the cells in 1ml of lysis buffer (50
279 mM Tris-HCl, 0.1% (v/v) Triton X-100, 200 mM NaCl, 1 mM DTT, 2mM EDTA) and keeping
280 them on ice for 30 minutes. Cells were disrupted in 3 x 60 second cycles using a FastPrep24
281 (MP Biomedicals, USA) and the debris were removed by centrifugation at 16000 x *g* for 15
282 minutes. Supernatants containing proteins were transferred into low bind protein tubes and
283 the proteins were quantified using Bradford's method (Bradford 1976).
284
285 Because estimation of cellulose degradation requires analyzing the total content of a sample
286 to be accurate, the measurements were performed on individual cultures that were prepared
287 separately. A collection of 18 bottles (9 time points in duplicate) were prepared using the
288 same inoculum described above, and grown in parallel with the 27-bottle collection used for
289 the meta-omic analyses. For each time point, the entire sample was recovered, centrifuged
290 at 5000 x *g* for 5 minutes and the supernatant was discarded. The resulting pellets were
291 boiled under acidic conditions as previously described (Zhou *et al.,* 2014) and the dried
292 weights, corresponding to the remaining cellulose, were measured.
293

294 mRNA extraction was performed in triplicate on time points T2 to T8, using previously
295 described methods (Gifford *et al.,* 2011) with the following modifications in the processing
296 of the RNA. The extraction of the mRNA included the addition of an *in vitro* transcribed RNA
297 as an internal standard to estimate the number of transcripts in the natural sample
298 compared with the number of transcripts sequenced. The standard was produced by the
299 linearization of a pGem-3Z plasmid (Promega, USA) with ScaI (Roche, Germany). The linear
300 plasmid was purified with a phenol/chloroform/isoamyl alcohol extraction and digestion of
301 the plasmid was assessed by agarose gel electrophoresis. The DNA fragment was transcribed
302 into a 994nt long RNA fragment with the Riboprobe *in vitro* Transcription System (Promega,
303 USA) following the manufacturer's protocol. Residual DNA was removed using the Turbo
304 DNA Free kit (Applied Biosystems, USA). The quantity and the size of the RNA standard was
305 measured with a 2100 bioanalyzer instrument (Agilent).
306
307 Total RNA was extracted using enzymatic lysis and mechanical disruption of the cells and
308 purified with the RNeasy mini kit following the manufacturer's protocol (Protocol 2, Qiagen,
309 USA). The RNA standard (25ng) was added at the beginning of the extraction in every
310 sample. After purification, residual DNA was removed using the Turbo DNA Free kit, and free
311 nucleotides and small RNAs such as tRNAs were cleaned off with a lithium chloride
312 precipitation solution according to ThermoFisher Scientific's recommendations. To reduce
313 the amount of rRNAs, samples were treated to enrich for mRNAs using the MICROBExpress
314 kit (Applied Biosystems, USA). Successful rRNA depletion was confirmed by analyzing both
315 pre- and post-treated samples on a 2100 bioanalyzer instrument. Enriched mRNA was
316 amplified with the MessageAmp II-Bacteria Kit (Applied Biosystems, USA) following
317 manufacturer's instruction and sent for sequencing at the Norwegian Sequencing Center
318 (NSC, Oslo, Norway). Samples were subjected to the TruSeq stranded RNA sample
319 preparation, which included the production of a cDNA library, and sequenced with paired-
320 end technology (2x125bp) on one lane of a HiSeq 3000 system.
321
322 RNA reads were assessed for overrepresented features (adapters/primers) using FastQC
323 (www.bioinformatics.babraham.ac.uk/projects/fastqc/), and ends with detected features
324 and/or a Phred score lower than 20 were trimmed using Trimmomatic v.0.36 (Bolger *et al.,*

325 2014). Subsequently, a quality filtering was applied with an average Phred threshold of 30
326 over a 10nt window and a minimum read length of 100nt. rRNA and tRNA were removed
327 using SortMeRNA v.2.1b (Kopylova *et al.,* 2012). SortMeRNA was also used to isolate the
328 reads originating from the pGem-3Z plasmid. These reads were mapped against the specific
329 portion of the plasmid containing the Ampr gene using Bowtie2 (Langmead 2012) with
330 default parameters and the number of reads per transcript was quantified. The remaining
331 reads were pseudoaligned against the metagenomic dataset, augmented with the annotated
332 strains, using Kallisto pseudo –pseudobam (Bray *et al.,* 2016). The resulting output was used
333 to generate mapping files with bam2hits, which were used for expression quantification with
334 mmseq (Turro *et al.,* 2011). Of the 40126 ORFs identified from the assembled SEM1b
335 metagenome and two *C. proteolyticus* strains, 16060 (40%) were not found to be expressed,
336 whereas 21482 (54%) were expressed and could be reliably quantified due to unique hits
337 (reads mapping unambiguously against one unique ORF) (**Figure S1A**). The remaining 2584
338 ORFs (6%) were expressed, but identified only with shared hits (reads mapping
339 ambiguously against more than one ORF, resulting in an unreliable quantification of the
340 expression of each ORF) (**Figure S1B**). Since having unique hits improves the expression
341 estimation accuracy, the ORFs were grouped using mmseq in order to improve the precision
342 of expression estimates, with only a small reduction in biological resolution (Turro *et al.,*
343 2014). The process first collapses ORFs into expression groups if they have 100% sequence
344 identity and then further collapses ORFs (or expression groups) if they acquire unique hits
345 as a group (**Figure S1C**). This process generated 39242 expression groups of which 38535
346 (98%) were singletons (groups composed of single ORF) and 707 (2%) were groups
347 containing more than one homologous ORF. From the initial 2584 low-information ORFs,
348 1333 became part of an expression group containing unique hits, 116 became part of
349 ambiguous group (no unique hits) and 1135 remained singletons (without unique hits). All
350 expression groups without unique hits were then excluded from the subsequent analysis. A
351 total of 21482 singletons and 594 multiple homologous expression groups were reliably
352 quantified between *BWF2A*, *SW3C* and the SEM1b metatranscriptome (**Figure S1C**).
353
354 In order to normalize the expression estimates, sample sizes were calculated using added
355 internal standards, as described previously (Gifford *et al.,* 2011). The number of reads

356 mapping on the defined region of the internal standard molecule were calculated to be
357 2.2x10^7 +/- 2.2x10^6 reads per sample out of 6.2x10^9 molecules added. Using this
358 information, the estimated number of transcript molecules per sample was computed to be
359 5.1x10^12 +/- 3.7x10^12 transcripts. The resulting estimates for the sample sizes were used
360 to scale the expression estimates from mmseq collapse and to obtain absolute expression
361 values. During initial screening the sample T7C (time point T7, replicate C) was identified as
362 an outlier using principle component analysis (PCA) and removed from downstream
363 analysis.
364
365 The expression groups were clustered using hierarchical clustering with Euclidean distance.
366 Clusters were identified using the Dynamic Tree Cut algorithm (Langfelder *et al.,* 2008) with
367 hybrid mode, deepsplit=1 and minClusterSize=7. Eigengenes were computed for the clusters
368 and clusters with a Pearson Correlation Coefficient (PCC) greater than 0.8 were merged. The
369 MAG/strain enrichment of the clusters was assessed using the BiasedUrn R package. The p-
370 values were corrected with the Benjamini-Hochberg procedure and the significance
371 threshold was set to 0.01. Expression groups composed of multiple MAGs/strains were
372 included in several enrichment tests.
373
374 **RESULTS AND DISCUSSION**
375 ***The SEM1b consortium is a simplistic community, co-dominated by Clostridium***
376 ***thermocellum and heterogeneic C. proteolyticus strains***
377 Molecular analysis of a reproducible, cellulose-degrading and biogas-producing consortium
378 (SEM1b) revealed a stable and simplistic population structure that contained approximately
379 seven populations, several of which consisted of multiple strains (**Figure 2**, **Table S2-S3**).
380 16S rRNA gene analysis showed that the SEM1b consortium was co-dominated by OTUs
381 affiliated to the genera *Clostridium* (52%) and *Coprothermobacter* (41%), with closest
382 representatives identified as *Clostridium (Ruminiclostridium) thermocellum,* an
383 uncharacterized *Clostridium spp.* and three *Coprothermobacter* phylotypes (**Table S2**).
384 Previous meta-omic analysis on the parent Frevar reactor, revealed a multitude of
385 numerically dominant *C. proteolyticus* strains, which created significant assembly and
386 binning related issues (Hagen *et al.,* 2017). In this study, multiple oligotypes of *C.*

proteolyticus were also found (**Table S2**). We therefore sought to isolate and recover axenic representatives to complement our meta-omic approaches, and using traditional anaerobic isolation techniques, we were successful in recovering two novel axenic strains (hereafter referred to as *BWF2A* and *SW3C*). The genomes of *BWF2A* and *SW3C* were sequenced and assembled and subsequently incorporated into our metagenomic and metatranscriptomic analysis below.

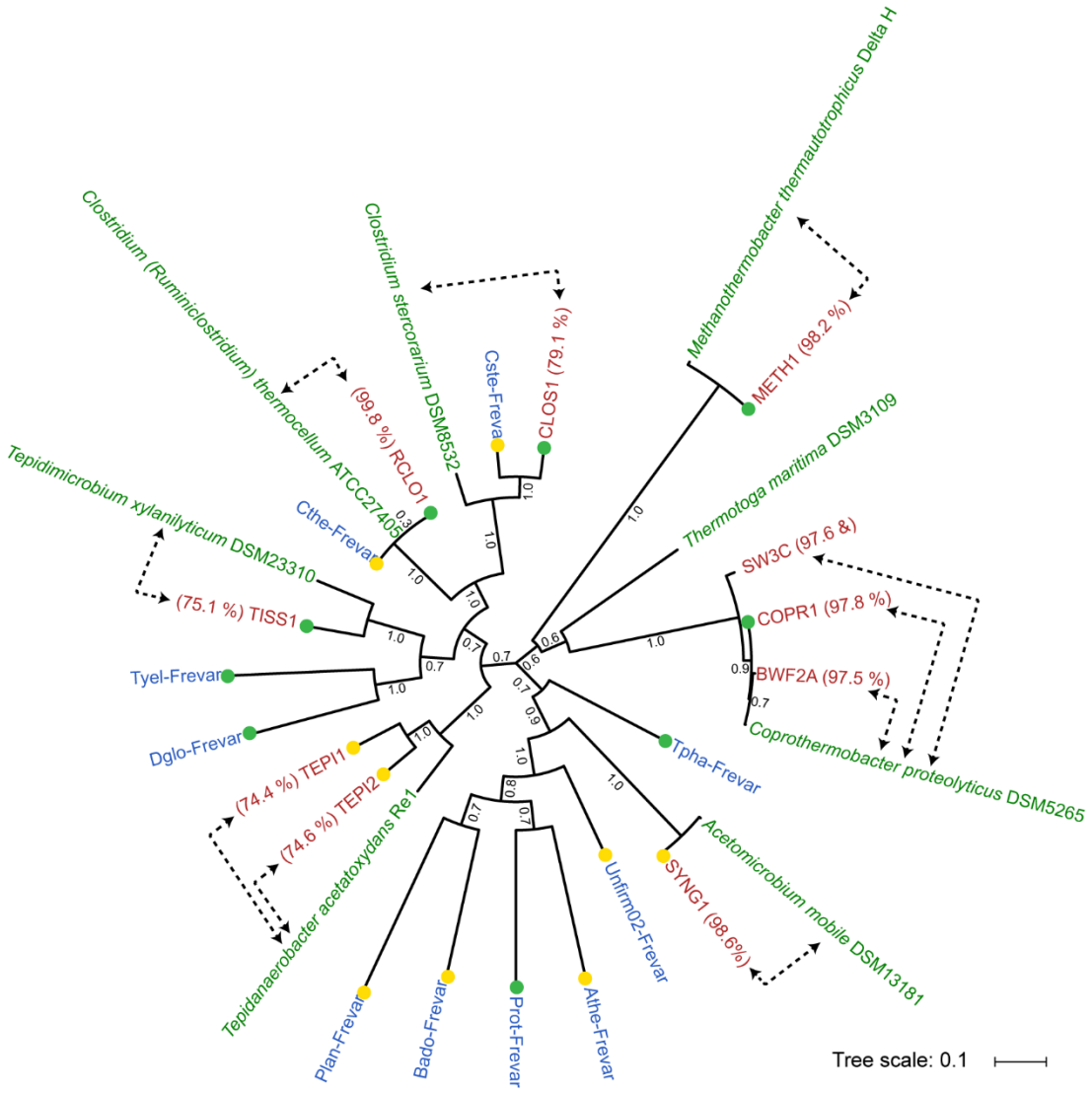

Figure 2. Phylogeny of *C. proteolyticus* strains and other MAGs recovered from the SEM1b consortium. Concatenated ribosomal protein tree of reference isolate genomes (green), MAGs from the previous Frevar study (blue, Hagen et al., 2017) and MAGs and isolate genomes recovered in this study (red). Average nucleotide identities (percentage indicated in parenthesis) were generated between SEM1b MAGs and their closest relative (indicated by dotted arrows). Bootstrap values are based on 1000 bootstrap replicates and the completeness of the MAGs are indicated by green (>90 %) and yellow (>80 %) colored dots.

400 Shotgun metagenome sequencing of two SEM1b samples (D1B and D2B), generated 290Gb
401 (502M paired-end reads) and 264Gb (457M paired-end reads) of data, respectively. Co-
402 assembly of both datasets using strain-depleted reads with Metaspades produced 20760
403 contigs totalizing 27Mbp with a maximum contig length of 603Kbp. Functional annotation
404 resulted in 36292 annotated ORFs and taxonomic binning revealed 11 MAGs and a
405 community structure similar to the one observed by 16S analysis (**Figure 2**, **Table S3**). A
406 total of eight MAGs exhibited good completeness > 80% and a low level of contamination (<
407 10%). Three MAGs, COPR2, COPR3 and SYNG2 corresponded to small and incomplete MAGs,
408 although Blastp analysis suggest COPR2 and COPR3 likely represent *Coprothermobacter*-
409 affiliated strain elements.
410
411 All near-complete MAGs (> 80%) as well as *BWF2A* and *SW3C* were phylogenetically
412 compared against their closest relatives using average nucleotide identities (ANI) and a
413 phylogenomic tree was constructed via analysis of 16 concatenated ribosomal proteins
414 (**Figure 2**). The COPR1 MAG was observed to cluster together with *C. proteolyticus* DSM 5265
415 and the two strains *BWF2A* and *SW3C.* Two MAGs (RCLO1-CLOS1) clustered together within
416 the *Clostridium*; RCLO1 with the well-known *C. thermocellum*, whereas CLOS1 grouped
417 together with another *Clostridium* MAG generated from the FREVAR dataset and the isolate
418 *C. stercorarium* (ANI: 79.1%). Both RCLO1 and CLOS1 encoded broad plant polysaccharide
419 degrading capabilities, containing 290 and 160 carbohydrate-active enzymes (CAZymes),
420 respectively (**Table S4**). RCLO1 in particular encoded cellulolytic (e.g. glycosyl hydrolase
421 (GH) families GH5, GH9, GH48) and cellulosomal features (dockerins and cohesins), whereas
422 CLOS1 appears more specialized towards hemicellulose degradation (e.g. GH3, GH10, GH26,
423 GH43, GH51, GH130). Surprisingly, CAZymes were also identified in COPR1 (n=30) and both
424 *BWF2A* (n=37) and *SW3C* (n=33) at levels higher than what has previously been observed in
425 *C. proteolyticus* DSM 5265 (n=14) (**Table S4**). Several MAGs were also affiliated with other
426 known lineages associated with biogas processes, including *Tepidanaerobacter* (TEPI1-2),
427 *Synergistales* (SYNG1-2), *Tissierellales* (TISS1) and Methanothermobacter (METH1).
428

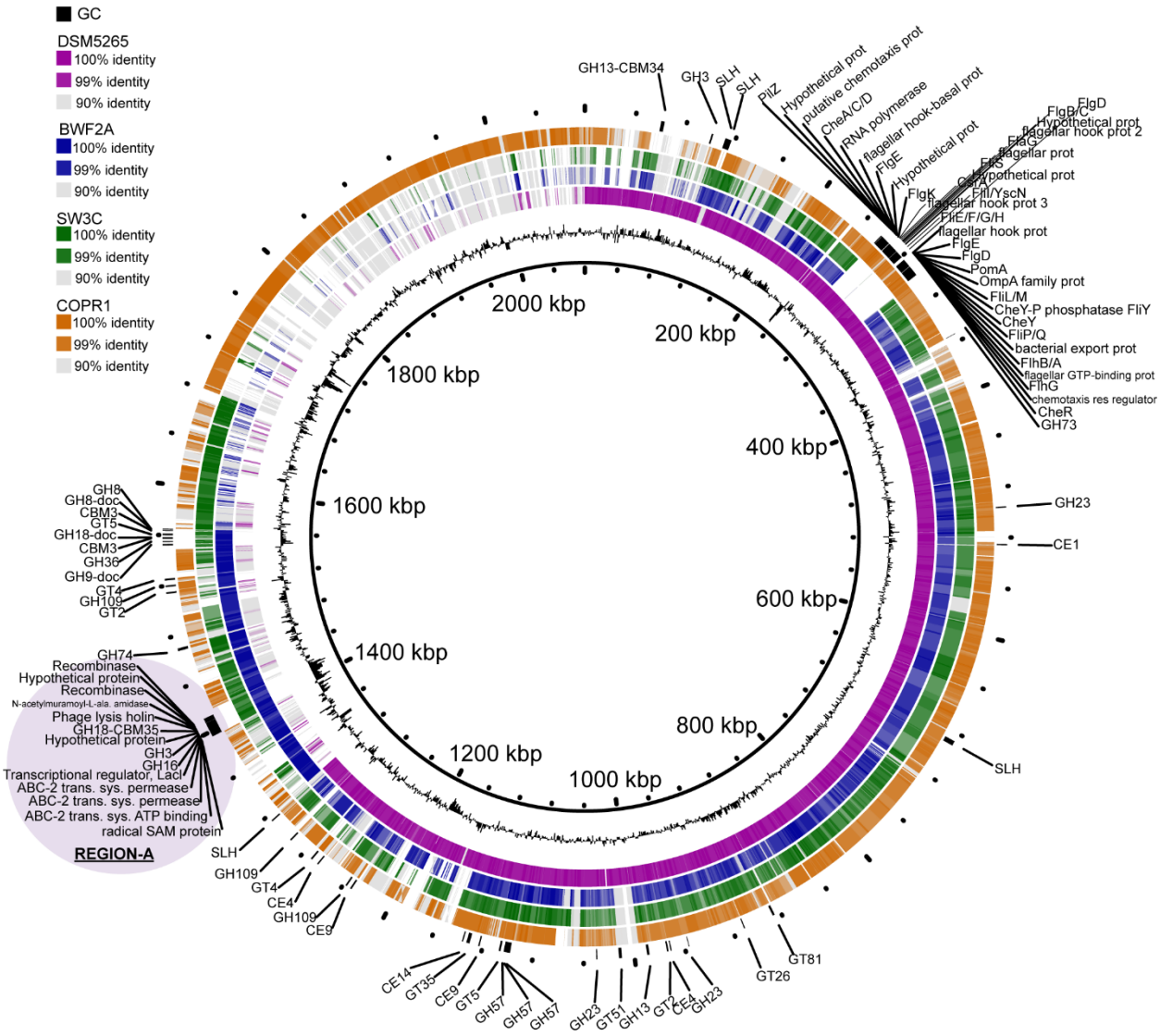

Figure 3. Comparative genome content of *C. proteolyticus* representatives including isolated strains, a recovered MAG (COPR1) and the reference strain DSM 5265. The innermost ring corresponds to the pangenome of the three *C. proteolyticus* spp. genomes and one MAG as produced by Roary (Page et al., 2015) and the second innermost ring represents the GC content. Outer rings represent the reference strain DSM 5265 (purple), the isolated strains BWF2A (blue) and SW3C (green) and the recovered COPR1 MAG (orange). Genes coding for carbohydrate-active enzymes (CAZymes) and flagellar proteins are indicted in black on the outermost ring. Genomic region-A is indicated by purple shading.

Novel strains of C. proteolyticus reveal acquisition of carbohydrate-active enzymes

Genome annotation of COPR1, *BWF2A* and *SW3C* identified both insertions and deletions in comparison to the only available reference genome, sequenced from the type strain DSM 5265 (**Figure 3**). Functional annotation showed that most of the genomic differences were

442 sporadic and are predicted not to affect the metabolism of the strains. However, several
443 notable differences were observed, which might represent a significant change in the
444 lifestyle of the isolates. Both isolated strains lost the genes encoding flagellar proteins, while
445 in contrast, they both acquired numerous extra CAZymes. Although both strains encoded a
446 slightly different collection of CAZymes, they both contained a particular genomic region that
447 encoded a cluster of three CAZymes: GH16, GH3 and GH18-CBM35 (region-A, **Figure 3**).
448 Other notable CAZy families found throughout the genome included GH36, GH74, GH109,
449 CBM3, CE1 and CE10 as well as GH9, GH8 and GH18 domains co-located with a dockerin. The
450 putative function of these GHs, suggests that both *BWF2A* and *SW3C* are capable of
451 hydrolyzing amorphous forms of cellulose (GH9: endoglucanase, CBM3: cellulose-binding)
452 and/or different hemicellulosic substrates (GH16: endo-1,3(4)-β-glucanase / xyloglucanase;
453 GH3: β-glucosidase / 1,4-β-xylosidase; GH36: α-galactosidase) (Álvarez *et al.,* 2016), which
454 are significant fractions of the spruce-derived cellulose substrate (glucan: 88.3%, xylan:
455 4.5%, mannan: 4.8%, (Chylenski *et al.,* 2017)). Regarding the putative GH18s encoded in both
456 strains (2 ORFs, with and without a dockerin), it could play a role in bacterial cell wall
457 recycling (Johnson *et al.,* 2013) as an endo-β-N-acetylglucosaminidase. Indeed, *C.*
458 *proteolyticus* has previously been considered to be a scavenger of dead cells, even though
459 this feature was mainly highlighted in term of proteolytic activities (Lü *et al.,* 2014).
460
461 Taking a closer look, the region-A of CAZymes (GH16, GH3, GH18-CBM35) in *BWF2A* and
462 *SW3C* was located on the same chromosomal cassette but organized onto two different
463 operons with opposite directions (**Figure S2A**). Comparison of the genes and their
464 organization, revealed a high percentage of gene similarity and synteny with genome
465 representatives of *Fervidobacterium nodosum* (Phylum: Thermotogae) and *C. thermocellum*
466 (**Table S5**). Both populations were previously identified in the original Frevar reactor
467 (Hagen *et al.,* 2017), and *C. thermocellum* representatives are also found in SEM1b (RCLO1).
468 Examination of the flanking regions surrounding the CAZymes in region-A, reveals the
469 presence of an incomplete prophage composed of a phage lysis holin and two recombinases
470 located downstream (**Figure 3, Figure S2A**). Further comparisons with *F. nodosum* and *C.*
471 *thermocellum* illustrated that only the later encodes the same prophage elements, together
472 with an additional terminase and more phage component proteins on the 5' region (**Figure**

473 **S2B**). Aside from region-A, most CAZymes encoded within *BWF2A* and *SW3C* genomes also
474 exhibited high similarity to representatives from *C. thermocellum* (**Table S5**). Considering
475 the high sequence homology and presence of phage-genes, it could be hypothesized that
476 genomic regions encoding CAZymes in *BWF2A* and *SW3C* are the result of HGT originating
477 from *C. thermocellum* and *F. nodosum*. HGT within anaerobic digesters has been reported for
478 antibiotic resistance genes (Miller *et al.,* 2016), whereas HGT of CAZymes have been detected
479 previously among gut microbiota (Hehemann *et al.,* 2010, Ricard *et al.,* 2006, Song *et al.,*
480 2016). Since many microbes express only a specific array of carbohydrate-degrading
481 capabilities, bacteria that acquire CAZymes from phages may gain additional capacities and
482 consequently, a selective growth advantage (Modi *et al.,* 2013).
483
484 Interestingly, several *BWF2A* and *SW3C* CAZymes were found to encode a GH domain
485 coupled with a dockerin (GH-doc) (**Table S5**), which are typical building block of
486 cellulosomes. Cellulosomes are multi-enzyme complexes produced by anaerobic cellulolytic
487 bacteria for the degradation of lignocellulosic biomass, and were first discovered in *C.*
488 *thermocellum* (Lamed et al., 1983). These complexes are composed of two main types of
489 building blocks: dockerin-containing enzymatic subunits and cohesin-containing structural
490 proteins called scaffoldins (Artzi *et al.,* 2017). Surprisingly, no cohesins were detected in
491 *BWF2A* or *SW3C*. Dockerin-only containing genomes have previously been observed,
492 however they remain poorly understood (Dassa *et al.,* 2014). In addition to cellulosome
493 building blocks, examination of the genome regions flanking a GH8 encoded in *BWF2A* (GH8,
494 IMG geneID: 2731989313), revealed both anti-sigma and RNA polymerase sigma factors
495 (**Figure S3**). Previous studies have shown that cellulosomal genes are regulated by anti-
496 sigma factors and alternative sigma factors in a substrate-dependent way (Artzi *et al.,* 2017,
497 Nataf *et al.,* 2010), and are unique to *C. thermocellum (Kahel-Raifer et al., 2010)*. The anti-
498 sigma system encoded upstream to the *BWF2A* GH8 exhibited 99% sequence identity to the
499 corresponding *C. thermocellum* genes that harbor the same gene organization (**Figure S3**).
500 Together, the high gene similarity, and presence of GH-doc domains and the anti-sigma
501 factors supports our previous assertions that many of the GHs present in *BWF2A* and *SW3C*
502 originated from *C. thermocellum*. Since the anti-sigma factor has an exocellular CBM-like
503 component to detect the presence of a particular substrate, it is tempting to speculate that

504 GHs from *C. proteolyticus* could be expressed and bind the complementary cohesin modules
505 produced by *C. thermocellum.*
506
507 ***C. proteolyticus expresses CAZymes and is implicit in polysaccharide degradation within***
508 ***the SEM1b consortium***
509 To better understand the role(s) played by *C. proteolyticus* in a saccharolytic consortium, a
510 temporal metatranscriptomic analyses of SEM1b over a complete life cycle was performed.
511 16S rRNA gene analysis of eight time points (T1-8) over a 43hr period reaffirmed that *C.*
512 *thermocellum*- and *C. proteolyticus*-affiliated populations dominate SEM1b over time (**Figure**
513 **4A**). Highly similar genes from different MAGs/genomes were grouped together in order to
514 obtain "expression groups" with discernable expression profiles (see **Methods** and **Figure**
515 **S1A/B**). A total of 408 singleton CAZyme expression groups and 13 multiple ORF groups
516 were collectively detected in the two *C. proteolyticus* strains and MAGs suspected of
517 contributing to polysaccharide degradation (RCLO1, CLOS1, COPR1-3, and TISS1, **Figure**
518 **S1D**, **Table S6**). In several instances, expressed CAZymes from *BWF2A* and *SW3C* could be
519 distinguished from their original sources (i.e. *C. thermocellum* and/or *F. nodosum*), but could
520 not be resolved between the two strains and/or the COPR1 MAG. For example, all GHs within
521 region-A could be identified as expressed by at least one of the isolated strains but could not
522 be resolved further between the strains. In contrast, the GH9-doc and GH8-doc ORFs were
523 unambiguously expressed and could not be resolved between *BWF2A* and *SW3C* and the
524 RCLO1 MAG, whereas GH8, GH18 and CBM3 ORFs were expressed by at least one of the *C.*
525 *proteolyticus* strains but could not be resolved further.
526
527 From the CAZymes subset of expression groups, a cluster analysis was performed to reveal
528 eight expression clusters (I-VIII, **Figure 4B**). Clusters I and II comprised 13 and 10
529 expression groups (respectively) and followed a similar profile over time (**Figure 4C**),
530 increasing at earlier stages (T2-3) and again at later stationary/death stages (T6-8). Both
531 clusters were enriched for *C. proteolyticus*-affiliated MAGs and isolated strains and
532 predominately consisted of CAZymes targeting linkages associated with N-
533 acetylglucosamine (CE9, CE14), peptidoglycan (GH23, GH18, GH73) and chitosan (GH8),
534 suggesting a role in bacterial cell wall hydrolysis (**Table S6**). This hypothesis was supported

535 by 16S rRNA gene data, which illustrated that *C. proteolyticus*-affiliated populations (OTU2)
536 were high at initial stages of the SEM1b life-cycle when cell debris was likely present in the
537 inoculum that was sourced from the preceding culture at stationary phase (**Figure 4A**). At
538 T2, the abundance of *C. thermocellum*-affiliated populations (OTU-1) was observed to
539 outrank *C. proteolyticus* as the community predictably shifted to cellulose-utilization.
540 However, towards stationary phase (T6-8) when dead cell debris is expected to be
541 increasing, expression levels in clusters I and II were maintained at high levels (**Figure 4B**),
542 which was consistent with high *C. proteolyticus* 16S rRNA gene abundance at the same time-
543 points.
544
545 Cluster IV, which was the second largest with 161 expression groups, was enriched with the
546 RCLO1 MAG that was closely related to *C. thermocellum*. As expected, numerous expressed
547 genes in cluster IV were inferred in cellulosome assembly (via cohesin and dockerin
548 domains) as well as cellulose (e.g. GH5, GH9, GH44, GH48, CBM3) and hemicellulose (e.g.
549 GH10, GH26, GH43, GH74) hydrolysis (**Table S6**). This cluster was increasing throughout the
550 consortium's exponential phase (time points T1-4, **Figure 4A**), whilst 16S rRNA data also
551 shows *C. thermocellum*-affiliated populations at high levels during the same stages (**Figure**
552 **4A**). Interestingly, the *BWF2A* and *SW3C* GH18-doc was also found in cluster IV. A GH9-doc
553 and GH8-doc encoded in *BWF2A* and *SW3C* were also expressed, however they exhibited 99-
554 100% identity to *C. thermocellum* representatives (**Table S5**) and formed expression groups
555 without unique hits, hence they were not part of the clustering (**Table S6**). Since
556 cellulosomal genes are seemingly expressed collectively in order to facilitate coordinated
557 assembly, finding the GH18 in the same cluster is not overly surprising. However, the fact
558 that the gene is expressed by a different bacterium to the one creating the bulk of the
559 cellulosome machinery (i.e. RCLO1) makes it extremely interesting and supports the
560 possibility that "multi-species" cellulosomes putatively exist. Although species-specific high-
561 affinity cohesin-dockerin interactions are required for cellulosome assembly (Pagès *et al.,*
562 1997), the *C. thermocellum*-origin and high homology of the *C. proteolyticus* GH18 gene lends
563 itself to the hypothesis that once expressed, the GH18 will bind to a RCLO1 cohesin domain
564 and be part of the resulting cellulosomes. Obviously, much more experimental validation is

565 required to confirm physical interactions between *C. proteolyticus* GH-doc representatives
566 and cellulosome assemblies.
567

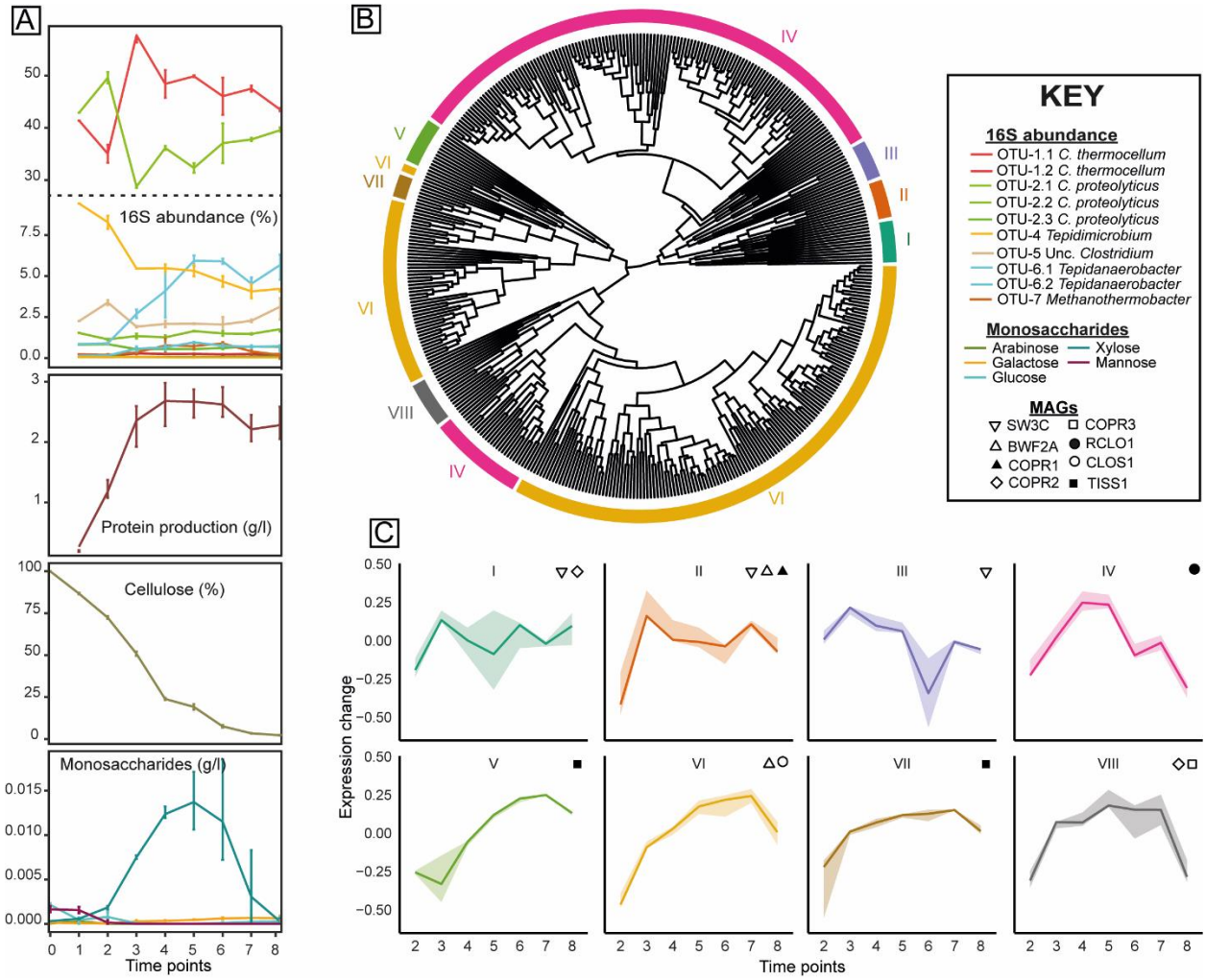

568

569 **Figure 4. Temporal meta-analysis of the SEM1b consortium.** (A) 16S rRNA gene amplicon and metadata
570 analysis was performed over a 43-hour period, which was segmented into 9 time-points. OTU IDs are detailed
571 in **Table S2**. Cellulose degradation rate, monosaccharide accumulation and growth rate (estimated by total
572 protein concentration) is presented. (B) Gene expression dendrogram and clustering of CAZymes from BWF2A,
573 SW3C and MAGs: RCLO1, CLOS1, COPR1-3, and TISS1. Eight expression clusters (I-VIII) are displayed in
574 different colors on the outer ring. (C) Clusters I-VIII show characteristic behaviors over time summarized by
575 the median (solid line) and the shaded area between the first and third quartile of the standardized expression.
576 Bacteria that are statistically enriched (p-value < 0.01) in the clusters are displayed in the subpanels.
577

578 ORFs from both *BWF2A* and *SW3C* as well as CLOS1 were enriched in cluster VI, which was
579 determined as the largest with 193 expression groups. CLOS1 in particular expressed many

genes involved in hemicellulose deconstruction (e.g. GH3, GH5, GH10, GH29, GH31, GH43 and GH130) and carbohydrate deacetylation (e.g. CE1, CE4, CE7, CE9, CE12) (**Table S6**). Expressed cluster VI genes from *C. proteolyticus* -affiliated genomes/MAGs were also inferred in hemicellulose-degradation, including GH3, GH16, GH74, CE1, CE4, CE9 and CE10 (**Table S6**). In particular, the GH16 and GH3-encoding ORFs from region-A within *BWF2A* and *SW3C* were detected in cluster VI, which reaffirms our earlier predictions that certain *C. proteolyticus* populations in SEM1b are capable of degrading hemicellulosic substrates. The expression profile of cluster VI over time was observed to slightly lag after cluster IV (**Figure 4**), suggesting that hemicellulases in cluster VI genes are expressed once the hydrolytic effects of the RCLO1-cellulosome (expressed in cluster IV) have liberated hemicellulosic substrates (Zverlov *et al.,* 2005b). Although *C. thermocellum* cannot readily utilize other carbohydrates besides cellodextrins (Demain *et al.,* 2005), the cellulosome is composed of a number of hemicellulolytic enzymes such as GH10 endoxylanases, GH26 mannanases and GH74 xyloglucanases (Zverlov *et al.,* 2005a), which are involved in the deconstruction of the underlying cellulose-hemicellulose matrix (Zverlov *et al.,* 2005b). Representatives of GH10, GH26 and GH74 from RCLO1 were all expressed in cluster IV and are presumably acting on the hemicellulose fraction present in the spruce-derived cellulose (Chylenski *et al.,* 2017). Furthermore, detection of hydrolysis products (**Figure 4A**), revealed that xylose increased significantly at T5-7, indicating that hemicellulosic polymers containing beta-1-4-xylan were likely available at these stages. In addition to cluster VI, clusters V, VII and VIII also exhibited expression profiles that gradually increased after the initial peak of cluster IV. These clusters were all found to contain many enzymes putatively targeting medium and short length carbohydrate chains, including those derived from xylan sources (**Table S6**).

All in all, the SEM1b expression data shows sequential community progression that co-ordinates hydrolysis of cellulose and hemicellulose as well as carbohydrates that are found in the microbial cell wall. In particular, *C. proteolyticus* populations in SEM1b were suspected to play key roles degrading microbial cell wall carbohydrates as well as hemicellulosic substrates, possibly in cooperation or in parallel to other clostridium populations at the later stages of the SEM1b growth cycle. The detection and expression of *C. proteolyticus* -affiliated

610 GH-doc enzymes also raises intriguing questions regarding the possibility of multi-species
611 cellulosomes and their potential role in saccharolytic consortia.
612
613 **CONCLUSIONS**
614 Unraveling the interactions occurring in a complex microbial community composed of
615 closely related species or strains is an arduous task. Here, we have leveraged culturing
616 techniques, metagenomics and time-resolved metatranscriptomics to describe a novel *C.*
617 *proteolyticus* population that is comprised of closely related strains that have acquired sets
618 of CAZymes via HGT and putatively evolved to incorporate a saccharolytic lifestyle. The co-
619 expression patterns of *C. proteolyticus* CAZymes in clusters I and II supports the adaptable
620 role of this bacterium as a scavenger that is able to hydrolyze cell wall polysaccharides
621 during initial phases of growth and in the stationary / death phase, when available sugars
622 are low. Moreover, the acquisition of hemicellulases by *C. proteolyticus*, and their expression
623 in cluster VI at time points when hemicellulose is available, further enhances its metabolic
624 versatility and provides substantial evidence as to why this population dominates
625 thermophilic reactors on a global scale, even when substrates are poor in protein.
626
627 **DATA AVAILABILITY**
628 All sequencing reads have been deposited in the sequence read archive (SRP134228), with
629 specific numbers listed in **Table S7**. All microbial genomes are publicly available on JGI
630 under the analysis project numbers listed in **Table S7**.
631
632 **ACKNOWLEDGEMENTS**
633 We are grateful for support from The Research Council of Norway (FRIPRO program, PBP:
634 250479 / NorZymeD, VGHE: 221568), as well as the European Research Commission
635 Starting Grant Fellowship (awarded to PBP; 336355 - MicroDE). The sequencing service was
636 provided by the Norwegian Sequencing Centre (www.sequencing.uio.no), a national
637 technology platform hosted by the University of Oslo and supported by the "Functional
638 Genomics" and "Infrastructure" programs of the Research Council of Norway and the
639 Southeastern Regional Health Authorities.
640

641 **COMPETING INTERESTS**

642 The authors declare there are no competing financial interests in relation to the work
643 described.

644

645 **REFERENCES**

646 Alexiev A, Coil DA, Badger JH, Enticknap J, Ward N, Robb FT *et al* (2014). Complete Genome
647 Sequence of *Coprothermobacter proteolyticus* DSM 5265. *Genome Announcements* **2:**
648 e00470–14.
649
650 Alikhan NF, Petty NK, Ben Zakour NL, Beatson SA (2011). BLAST Ring Image Generator
651 (BRIG): Simple prokaryote genome comparisons. *BMC Genomics* **12:** 402.
652
653 Álvarez C, Reyes-Sosa FM, Díez B (2016). Enzymatic hydrolysis of biomass from wood.
654 *Microbial Biotechnology* **9:** 149-156.
655
656 Artzi L, Bayer EA, Moraïs S (2017). Cellulosomes: Bacterial nanomachines for dismantling
657 plant polysaccharides. *Nature Reviews Microbiology* **15:** 83-95.
658
659 Bendall ML, Stevens SLR, Chan LK, Malfatti S, Schwientek P, Tremblay J *et al* (2016). Genome-
660 wide selective sweeps and gene-specific sweeps in natural bacterial populations. *ISME*
661 *Journal* **10:** 1589-1601.
662
663 Biller SJ, Berube PM, Lindell D, Chisholm SW (2015). Prochlorococcus: The structure and
664 function of collective diversity. *Nature Reviews Microbiology* **13:** 13-27.
665
666 Bolger AM, Lohse M, Usadel B (2014). Trimmomatic: A flexible trimmer for Illumina
667 sequence data. *Bioinformatics* **30:** 2114-2120.
668
669 Bradford MM (1976). A rapid and sensitive method for the quantitation of microgram
670 quantities of protein utilizing the principle of protein-dye binding. *Analytical Biochemistry*
671 **72:** 248-254.
672
673 Bray NL, Pimentel H, Melsted P, Pachter L (2016). Near-optimal probabilistic RNA-seq
674 quantification. *Nature Biotechnology* **34:** 525-527.
675
676 Bron PA, Van Baarlen P, Kleerebezem M (2012). Emerging molecular insights into the
677 interaction between probiotics and the host intestinal mucosa. *Nature Reviews Microbiology*
678 **10:** 66-78.
679
680 Caporaso JG, Kuczynski J, Stombaugh J, Bittinger K, Bushman FD, Costello EK *et al* (2010).
681 QIIME allows analysis of high-throughput community sequencing data. *Nature methods* **7:**
682 335-336.
683

Chen IMA, Markowitz VM, Chu K, Palaniappan K, Szeto E, Pillay M *et al* (2017). IMG/M: Integrated genome and metagenome comparative data analysis system. *Nucleic Acids Research* **45:** D507-D516.

Chylenski P, Petrović DM, Müller G, Dahlström M, Bengtsson O, Lersch M *et al* (2017). Enzymatic degradation of sulfite-pulped softwoods and the role of LPMOs. *Biotechnology for Biofuels* **10:** 1-13.

Dassa B, Borovok I, Ruimy-Israeli V, Lamed R, Flint HJ, Duncan SH *et al* (2014). Rumen cellulosomics: Divergent fiber-degrading strategies revealed by comparative genome-wide analysis of six ruminococcal strains. *PLoS ONE* **9**.

Demain AL, Newcomb M, Wu JHD, Demain AL, Newcomb M, Wu JHD (2005). Cellulase, Clostridia, and Ethanol. *Microbiology and Molecular Biology Reviews* **69:** 124-154.

Edgar RC (2004). MUSCLE: Multiple sequence alignment with high accuracy and high throughput. *Nucleic Acids Research* **32:** 1792-1797.

Edgar RC (2010). Search and clustering orders of magnitude faster than BLAST. *Bioinformatics* **26:** 2460-2461.

Ellegaard KM, Engel P (2016). Beyond 16S rRNA community profiling: Intra-species diversity in the gut microbiota. *Frontiers in Microbiology* **7:** 1-16.

Etchebehere C, Pavan ME, Zorzópulos J, Soubes M, Muxí L (1998). Coprothermobacter platensis sp. nov., a new anaerobic proteolytic thermophilic bacterium isolated from an anaerobic mesophilic sludge. *International journal of systematic bacteriology* **48:** 1297-1304.

Gifford SM, Sharma S, Rinta-Kanto JM, Moran MA (2011). Quantitative analysis of a deeply sequenced marine microbial metatranscriptome. *ISME Journal* **5:** 461-472.

Gill SR, Fouts DE, Archer GL, Mongodin EF, Deboy RT, Ravel J *et al* (2005). Insights on Evolution of Virulence and Resistance from the Complete Genome Analysis of an Early Methicillin-Resistant Staphylococcus aureus Strain and a Biofilm-Producing Methicillin-Resistant Staphylococcus epidermidis Strain. *J Bacteriol* **187:** 2426-2438.

González-Torres P, Pryszcz LP, Santos F, Martínez-García M, Gabaldón T, Antón J (2015). Interactions between closely related bacterial strains are revealed by deep transcriptome sequencing. *Applied and Environmental Microbiology* **81:** 8445-8456.

Hagen LH, Frank JA, Zamanzadeh M, Eijsink VGH, Pope PB, Horn SJ *et al* (2017). Quantitative metaproteomics highlight the metabolic contributions of uncultured phylotypes in a thermophilic anaerobic digester. *Applied and Environmental Microbiology* **83**.

728 Hehemann JH, Correc G, Barbeyron T, Helbert W, Czjzek M, Michel G (2010). Transfer of
729 carbohydrate-active enzymes from marine bacteria to Japanese gut microbiota. *Nature* **464:**
730 908-912.
731
732 Hug LA, Baker BJ, Anantharaman K, Brown CT, Probst AJ, Castelle CJ *et al* (2016). A new view
733 of the tree of life. *Nature Microbiology* **1:** 1-6.
734
735 Hungate RE (1969). Chapter IV A Roll Tube Method for Cultivation of Strict Anaerobes. In:
736 Norris JR, Ribbons DWBTMiM (eds). *Methods in Microbiology*. Academic Press. pp 117-132.
737
738 Hunt DE, David LA, Gevers D, Preheim SP, Alm EJ, Polz MF (2008). Resource Partitioning and
739 Sympatric Differentiation Among Closely Related Bacterioplankton. *Science* **320:** 1081 LP-
740 1085.
741
742 Johnson JW, Fisher JF, Mobashery S (2013). Bacterial cell wall recycling. *Annals of the new*
743 *york academy* **1277:** 54-75.
744
745 Kahel-Raifer H, Jindou S, Bahari L, Nataf Y, Shoham Y, Bayer EA *et al* (2010). The unique set
746 of putative membrane-associated anti-σ factors in Clostridium thermocellum suggests a
747 novel extracellular carbohydrate-sensing mechanism involved in gene regulation. *FEMS*
748 *Microbiology Letters* **308:** 84-93.
749
750 Kang DD, Froula J, Egan R, Wang Z (2015). MetaBAT, an efficient tool for accurately
751 reconstructing single genomes from complex microbial communities. *PeerJ* **3:** e1165-e1165.
752
753 Kashtan N, Roggensack SE, Rodrigue S, Thompson JW, Biller SJ, Coe A *et al* (2014). Single-Cell
754 Genomics Reveals Hundreds of coexisting subpopulations in wild Prochlorococcus. *Science*
755 *(New York, NY)* **344:** 416-420.
756
757 Kopylova E, Noé L, Touzet H (2012). SortMeRNA: Fast and accurate filtering of ribosomal
758 RNAs in metatranscriptomic data. *Bioinformatics* **28:** 3211-3217.
759
760 Koskella B, Vos M (2015). Adaptation in Natural Microbial Populations. *Annual Review of*
761 *Ecology, Evolution, and Systematics* **46:** 503-522.
762
763 Kumar S, Stecher G, Tamura K (2016). MEGA7: Molecular Evolutionary Genetics Analysis
764 Version 7.0 for Bigger Datasets. *Molecular biology and evolution* **33:** 1870-1874.
765
766 Kunath BJ, Bremges A, Weimann A, McHardy AC, Pope PB (2017). Metagenomics and
767 CAZyme Discovery. In: Abbott DW, Lammerts van Bueren A (eds). *Protein-Carbohydrate*
768 *Interactions: Methods and Protocols*. Springer New York: New York, NY. pp 255-277.
769
770 Lamed R, Setter E, Bayer EA (1983). Characterization of a cellulose-binding, cellulase-
771 containing complex in Clostridium thermocellum. *Journal of Bacteriology* **156:** 828-836.
772

773 Langfelder P, Zhang B, Horvath S (2008). Defining clusters from a hierarchical cluster tree:
774 The Dynamic Tree Cut package for R. *Bioinformatics* **24:** 719-720.
775
776 Langmead (2012). Fast gapped-read alignment with Bowtie 2. *Nature methods* **9:** 357-359.
777
778 Letunic I, Bork P (2016). Interactive tree of life (iTOL) v3: an online tool for the display and
779 annotation of phylogenetic and other trees. *Nucleic acids research* **44:** W242-W245.
780
781 Li H (2013). Aligning sequence reads, clone sequences and assembly contigs with BWA-
782 MEM. *arxiv* **00:** 1-3.
783
784 Lü F, Bize A, Guillot A, Monnet V, Madigou C, Chapleur O *et al* (2014). Metaproteomics of
785 cellulose methanisation under thermophilic conditions reveals a surprisingly high
786 proteolytic activity. *ISME Journal* **8:** 88-102.
787
788 Martin M (2011). Cutadapt removes adapter sequences from high-throughput sequencing
789 reads. *EMBnetjournal* **17:** 10-10.
790
791 McLoughlin K, Schluter J, Rakoff-Nahoum S, Smith AL, Foster KR (2016). Host Selection of
792 Microbiota via Differential Adhesion. *Cell Host and Microbe* **19:** 550-559.
793
794 Miller JH, Novak JT, Knocke WR, Pruden A (2016). Survival of antibiotic resistant bacteria
795 and horizontal gene transfer control antibiotic resistance gene content in anaerobic
796 digesters. *Frontiers in Microbiology* **7:** 1-11.
797
798 Modi SR, Lee HH, Spina CS, Collins JJ (2013). Antibiotic treatment expands the resistance
799 reservoir and ecological network of the phage metagenome. *Nature* **499:** 219-222.
800
801 Nataf Y, Bahari L, Kahel-Raifer H, Borovok I, Lamed R, Bayer EA *et al* (2010). Clostridium
802 thermocellum cellulosomal genes are regulated by extracytoplasmic polysaccharides via
803 alternative sigma factors. *Proceedings of the National Academy of Sciences* **107:** 18646-
804 18651.
805
806 Nurk S, Meleshko D, Korobeynikov A, Pevzner PA (2017). MetaSPAdes: A new versatile
807 metagenomic assembler. *Genome Research* **27:** 824-834.
808
809 Ochman H, Lawrence JG, Grolsman EA (2000). Lateral gene transfer and the nature of
810 bacterial innovation. *Nature* **405:** 299-304.
811
812 Ollivier BM, Mah Ra, Ferguson TJ, Boone DR, Garcia JL, Robinson R (1985). Emendation of
813 the Genus Thermobacteroides: Thermobacteroides proteolyticus sp. nov., a proteolytic
814 acetogen from a methanogenic enrichment. *International Journal of Systematic Bacteriology*
815 **35:** 425-428.
816
817 Page AJ, Cummins CA, Hunt M, Wong VK, Reuter S, Holden MTG *et al* (2015). Roary: Rapid
818 large-scale prokaryote pan genome analysis. *Bioinformatics* **31:** 3691-3693.

Pagès S, Bélaïch A, Bélaïch J-P, Morag E, Lamed R, Shoham Y *et al* (1997). Species-specificity of the cohesin-dockerin interaction between Clostridium thermocellum and Clostridium cellulolyticum: Prediction of specificity determinants of the dockerin domain. *Proteins: Structure, Function, and Bioinformatics* **29:** 517-527.

Parks DH, Imelfort M, Skennerton CT, Hugenholtz P, Tyson GW (2015). CheckM: Assessing the quality of microbial genomes recovered from isolates, single cells, and metagenomes. *Genome Research* **25:** 1043-1055.

Ricard G, McEwan NR, Dutilh BE, Jouany JP, Macheboeuf D, Mitsumori M *et al* (2006). Horizontal gene transfer from bacteria to rumen ciliates indicates adaptation to their anaerobic, carbohydrates-rich environment. *BMC Genomics* **7:** 1-13.

Rodriguez-R LM, Konstantinidis KT (2016). The enveomics collection: a toolbox for specialized analyses of microbial genomes and metagenomes. *PeerJ Preprints* **4:** e1900v1901.

Rodriguez-Valera F, Martin-Cuadrado A-B, Rodriguez-Brito B, Pašić L, Thingstad TF, Rohwer F *et al* (2009). Explaining microbial population genomics through phage predation. *Nature Reviews Microbiology* **7:** 828-828.

Rosenzweig RF, Sharp RR, Treves DS, Adams J (1994). Microbial evolution in a simple unstructured environment: Genetic differentiation in Escherichia coli. *Genetics* **137:** 903-917.

Rødsrud G, Lersch M, Sjöde A (2012). History and future of world's most advanced biorefinery in operation. *Biomass and Bioenergy* **46:** 46-59.

Schloissnig S, Arumugam M, Sunagawa S, Mitreva M, Tap J, Zhu A *et al* (2013). Genomic variation landscape of the human gut microbiome. *Nature* **493:** 45-50.

Schumann P (1991). Nucleic Acid Techniques in Bacterial Systematics (Modern Microbiological Methods). *Journal of Basic Microbiology* **31:** 479-480.

Shapiro BJ, Timberlake SC, Szabó G, Polz MF, Alm EJ (2012). Population Genomics of Early Differentiation of Bacteria. *Science* **336:** 48-51.

Sharon I, Morowitz MJ, Thomas BC, Costello EK, Relman DA, Banfield JF (2013). Time series community genomics analysis reveals rapid shifts in bacterial species, strains, and phage during infant gut colonization. *Genome Research* **23:** 111-120.

Siezen RJ, Tzeneva VA, Castioni A, Wels M, Phan HTK, Rademaker JLW *et al* (2010). Phenotypic and genomic diversity of Lactobacillus plantarum strains isolated from various environmental niches. *Environmental Microbiology* **12:** 758-773.

Solheim M, Aakra Å, Snipen LG, Brede DA, Nes IF (2009). Comparative genomics of Enterococcus faecalis from healthy Norwegian infants. *BMC Genomics* **10:** 1-11.

Song T, Xu H, Wei C, Jiang T, Qin S, Zhang W *et al* (2016). Horizontal Transfer of a Novel Soil Agarase Gene from Marine Bacteria to Soil Bacteria via Human Microbiota. *Scientific Reports* **6:** 1-10.

Spanogiannopoulos P, Bess EN, Carmody RN, Turnbaugh PJ (2016). The microbial pharmacists within us: A metagenomic view of xenobiotic metabolism. *Nature Reviews Microbiology* **14:** 273-287.

Stoddard SF, Smith BJ, Hein R, Roller BRK, Schmidt TM (2015). rrnDB: Improved tools for interpreting rRNA gene abundance in bacteria and archaea and a new foundation for future development. *Nucleic Acids Research* **43:** D593-D598.

Takahashi S, Tomita J, Nishioka K, Hisada T, Nishijima M (2014). Development of a prokaryotic universal primer for simultaneous analysis of Bacteria and Archaea using next-generation sequencing. *PLoS ONE* **9**.

Tandishabo K, Nakamura K, Umetsu K, Takamizawa K (2012). Distribution and role of Coprothermobacter spp. in anaerobic digesters. *Journal of Bioscience and Bioengineering* **114:** 518-520.

Tettelin H, Masignani V, Cieslewicz MJ, Donati C, Medini D, Ward NL *et al* (2005). Genome analysis of multiple pathogenic isolates of Streptococcus agalactiae: Implications for the microbial "pan-genome". *Proceedings of the National Academy of Sciences* **102:** 13950-13955.

Treangen TJ, Rocha EPC (2011). Horizontal transfer, not duplication, drives the expansion of protein families in prokaryotes. *PLoS Genetics* **7**.

Truong DT, Tett A, Pasolli E, Huttenhower C, Segata N (2017). Microbial strain-level population structure & genetic diversity from metagenomes. *Genome Research* **27:** 626-638.

Turro E, Su SY, Gonçalves Â, Coin LJM, Richardson S, Lewin A (2011). Haplotype and isoform specific expression estimation using multi-mapping RNA-seq reads. *Genome Biology* **12:** 1-15.

Turro E, Astle WJ, Tavaré S (2014). Flexible analysis of RNA-seq data using mixed effects models. *Bioinformatics* **30:** 180-188.

Yin Y, Mao X, Yang J, Chen X, Mao F, Xu Y (2012). DbCAN: A web resource for automated carbohydrate-active enzyme annotation. *Nucleic Acids Research* **40:** 445-451.

Zamanzadeh M, Hagen LH, Svensson K, Linjordet R, Horn SJ (2016). Anaerobic digestion of food waste - Effect of recirculation and temperature on performance and microbiology. *Water Research* **96:** 246-254.

Zelezniak A, Andrejev S, Ponomarova O, Mende DR, Bork P, Patil KR (2015). Metabolic dependencies drive species co-occurrence in diverse microbial communities. *Proceedings of the National Academy of Sciences* **112:** 6449-6454.

Zhou Y, Pope PB, Li S, Wen B, Tan F, Cheng S *et al* (2014). Omics-based interpretation of synergism in a soil-derived cellulose-degrading microbial community. *Scientific Reports* **4:** 1-6.

Zunino P, Piccini C, Legnani-Fajardo C (1994). Flagellate and non-flagellate Proteus mirabilis in the development of experimental urinary tract infection. *Microbial Pathogenesis* **16:** 379-385.

Zverlov VV, Kellermann J, Schwarz WH (2005a). Functional subgenomics of Clostridium thermocellum cellulosomal genes: Identification of the major catalytic components in the extracellular complex and detection of three new enzymes. *Proteomics* **5:** 3646-3653.

Zverlov VV, Schantz N, Schmitt-Kopplin P, Schwarz WH (2005b). Two new major subunits in the cellusome of Clostridium thermocellum: Xyloglucanase Xgh74A and endoxylanase Xyn10D. *Microbiology* **151:** 3395-3401.